Proceedings 10th NUMGE 2023
10th European Conference on Numerical Methods in Geotechnical Engineering
Zdravkovic L, Kontoe S, Taborda DMG, Tsiampousi A (eds)

https://doi.org/10.53243/NUMGE2023-401

Numerical study on a pile subjected to seismic loading in crushable soil

Mohd Saqib[1], Arghya Das[1], Nihar Ranjan Patra[1]

[1]*Department of Civil Engineering, Indian Institute of Technology Kanpur, Uttar Pradesh, India*

ABSTRACT: The response of a pile embedded in crushable sand to earthquake loading is studied using finite elements. For this purpose, a bounding surface plasticity soil model is enhanced to include grain breakage via evolution in the critical state line. The adaptive Runge-Kutta-Fehlberg stress integration method is used for numerical implementation of the constitutive model. The model is implemented into the finite element programme (ABAQUS) as a user-defined material. The predictive ability of the improved model is tested against laboratory tests, and the pile response is validated using simulation results from the literature. The effect of particle breakage on the evolution of the pore water pressure ratio is investigated. According to the simulation results, particle crushing occurs primarily during the early stages of seismic excitation and increases pore water pressure, making the pile more prone to liquefaction. A significant increase in pore water pressure increases liquefaction susceptibility.

Keywords: Particle breakage; SANISAND; Liquefaction; Finite Element Model

1 INTRODUCTION

Numerical modelling of geo-structures has become increasingly popular in recent years as a result of widespread availability of computing facilities that accommodate a wide range of boundary conditions, and the development of more sophisticated material models (constitutive laws). For decades, scientists have attempted to predict soil behaviour under cyclic loading by developing a variety of constitutive models. (Bouckovalas et al. 2003; Dafalias and Manzari 2004; Liu et al. 2019; Petalas et al. 2019; Taiebat and Dafalias 2008). Any continuum-based numerical model, such as pile reaction under cyclic loading, requires an adequate material model and proper numerical stress integration. Rapidly increasing pore water pressure causes liquefaction, a condition of zero effective stress where shear strength diminishes and significant damage can occur. It is crucial to model pore water pressure accurately in to predict and avoid possible issues. (Wobbes et al. (2017) used UBC3D-PLM in a two-phase finite element method to model the liquefaction phenomenon (FEM). When compared to the experimental data, the model's prediction of excess pore water was observed to be slower. Galavi et al. (2013) utilized a similar model but with viscous boundaries to avoid boundary reflection. The model was unable to predict the sharp evolution of excess pore water pressure in anisotropic consolidated clay. Cheng and Jeremić (2009) used a bounding surface model to model the soil skeleton and a fully coupled dynamic formula to model the pore pressure. Few studies have utilised the unified model presented by Wang et al. (2014) within a critical state framework, with most attention given to modelling the behaviour of sand post liquefaction (Wang et al. 2016). Although the unified model underestimates sand re-consolidation settlement, it showed outstanding capabilities in simulating sand response to a wide range of densities and confining pressures. The majority of research, however, has focused on non-crushable siliceous sands.

According to few research, carbonate-rich sands like those found in Dog's Bay may crush at a relatively low stress (Wood and Maeda 2008). It is critical to include particle crushing in constitutive models to more accurately replicate the behaviour of crushable sand. Several studies have shown that particle crushing alters the critical state line (Hu et al. 2011; Tengattini et al. 2016; Wood and Maeda 2008). A small number of laboratory experiments demonstrated that particle breakage affects sand behaviour by causing a downward shift in the CSL in the e-p' space (Ghafghazi et al. 2014; Xiao et al. 2021).

A suitable material model is required to simulate pile behaviour under seismic or cyclic loading in crushable granular regions. As a result, further investigation is required to assess the effect of particle crushing on pile behaviour in crushable soils during earthquake loading. The SANISAND family of sand anisotropic models is one of the most versatile and widely used sand models in recent years for cyclic loading analysis. A variant of the SANISAND family (Dafalias and Manzari 2004; Liu et al. 2019; Manzari and Dafalias 1997; Petalas et al. 2019; Taiebat and Dafalias 2008; Yang et al. 2020) derives from the two-surface plasticity model developed

by Manzari and Dafalias (1997), which simulates soil behaviour under monotonic and cyclic loading. Upgrades to the SANISAND model (SS08 and SS04) with hyperbolic breakage have been implemented in a few recent research (Irani et al. 2022; Saqib et al. 2022). However, the performance of breakage augmented SANISAND in solving boundary value problems is not analysed in any of these research, only the constitutive response (single element) is evaluated.

A three-dimensional (3D) FEM model is presented to simulate pile behaviour in crushable soil subjected to seismic loading. To model the pore pressure evolution, an uncoupled pore pressure evolution (assuming fully undrained) is considered. The pile-soil interaction and the resulting liquefaction during crushing is investigated. This paper extends the constitutive model of Taiebat and Dafalias (2008) to account for the shift in the critical state line caused by grain breaking. Initially, the modified version is verified using the experiments conducted by Hyodo et al. (2017) on Aio sand, respectively. Based on simulations conducted for non-crushable soil by Cheng and Jeremić (2009), the FE model response is verified. Finally, the influence of particle crushing on an increase in the pore water pressure ratio is evaluated using a parametric investigation of the FE model during the earthquake time history.

2 MATERIAL MODEL

The critical state SANISAND (SS08) model, presented by Taiebat and Dafalias (2008) under the context of bounding surface plasticity, is used to characterise the mechanical behaviour of soil. This model's ability to predict plastic deformations under constant and variable stress ratio type loading is its most distinguishing feature over its predecessors. Figure 1 depicts a schematic representation of the SANISAND model in the deviatoric stress ratio plane. The SSO8 model is improved by incorporating particle breakage through the evolution of a change in the critical state line (CSL). The alteration occurs as a result of grain breakage caused by isotropic and deviatoric stresses during loading.

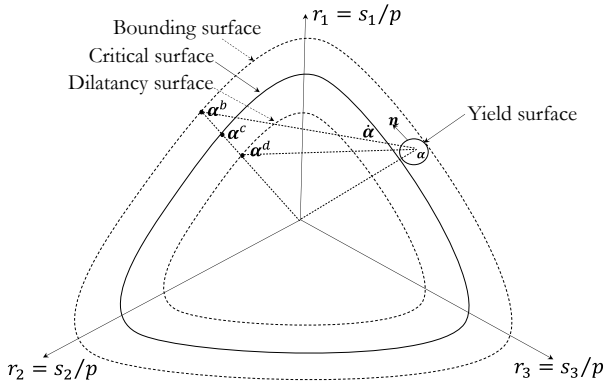

Figure 1. Schematic representation of the model surfaces and mapping rules of $\boldsymbol{\alpha}^{c,b,d}$ on the π plane.

For this purpose, Li and Wang (1998) equation is modified to account for particle breakage. The proposed equation by Li and Wang (1998) to determine the location of the CSL in the e-p' is given as:

$$e_c = e_{ref} - \lambda_c (p_c/p_{at})^{\xi} \tag{1}$$

where e_{ref} is the reference void ratio defined as a particular point on the CSL in the $e - logp$ plane. The hyperbolic equation derived by Hu et al. (2011) is adopted to modify the CSL equation by changing e_{ref} as

$$e_{ref} = e_{ref0} + \left(e_{refu} - e_{ref0}\right)\frac{B_r}{\rho + B_r} \tag{2}$$

where e_{ref0} and e_{refu} represent the initial and ultimate reference critical void ratios, respectively; ρ is the model parameter that controls the position of CSL in the $e - p'$ space and B_r is the relative breakage defined as the function of plastic work in the form

$$B_r = \frac{w_p}{\chi + w_p} \tag{3}$$

where χ is a constant indicating the crushing resistance of the granular material. w_p is the plastic work can be calculated as

$$w_p = \int p\langle \dot{\varepsilon}_v^p \rangle + q d\varepsilon_q^p \tag{4}$$

The Macaulay function in Equation (4) implies that dilation $(d\varepsilon_v^p < 0)$ is not accounted for breakage calculation since particles are going apart during volume expansion and eliminating the change of breakage. The response of the SS08-Breakage model to undrained cyclic loading is compared to the experimental test results obtained by Hyodo et al. (2017) . The proposed plasticity model requires parameter calibration using the procedure described in (Dafalias and Manzari 2004; Hu et al. 2011; Taiebat and Dafalias 2008).

The experimental results and model predictions for consoli-dated undrained cyclic tests on Aio sand samples at a confining pressure of 5MPa are shown in Figure 2. The nature of the stress strain plot is demonstrated in Figure 2(a), while Figure 2(b) compares the experimental measurement of breakage to its counterpart from the model prediction under undrained cyclic triaxial loading conditions. The proposed SS08-Breakage-breakage Model's estimation under cyclic loading agrees well with the experimental results. However, due to the lack of loading-induced anisotropy, the stress strain plot only qualitatively matches the experimental results.

.

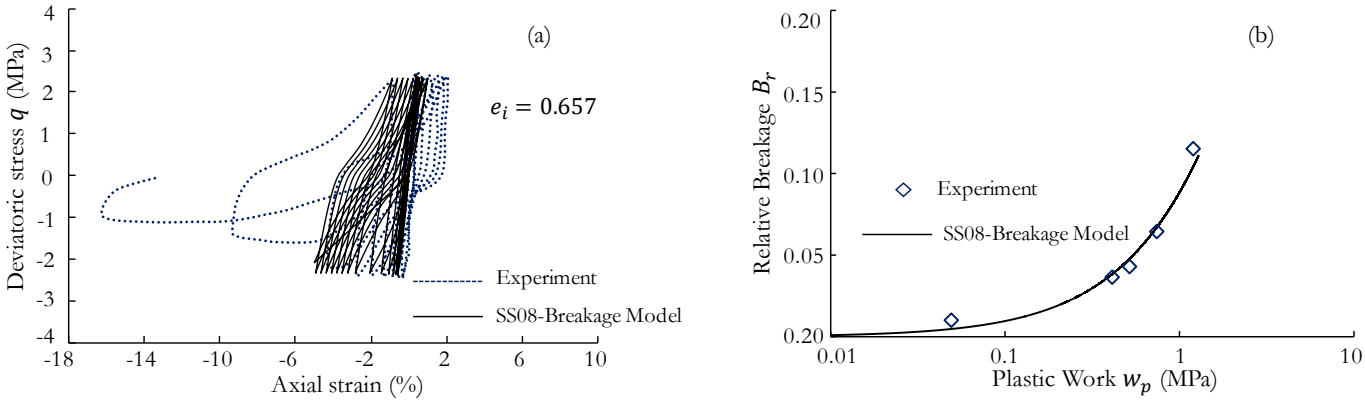

Figure 2. Consolidated undrained triaxial response of dense Aio sand: (a) stress-strain plot (b) Relative breakage evolution with initial void ratio of $e_i = 0.657$.

3 3D FINITE ELEMENT MODELLING OF PILE

To analyse the behaviour of the pile under seismic loading conditions, a boundary value problem is solved using finite elements (FE). The material model (breakage enhanced SS08) is implemented as a user-defined material (UMAT) model in ABAQUS. The Adaptive Runge Kutta Fehlberg Method (RKF-23), as presented by Sloan et al. (2001) is utilized for stress integration . For this simulation of a pile in liquefiable soil, the boundary value problem with the same geometry and discretization proposed by (Cheng and Jeremić 2009) is used. To reduce complexity, a 3D FEM model is developed on the assumption of totally undrained (uncoupled pore pressure evolution). The discretized model shown in Figure 3 along with acceleration time history. Half of a soil block and a pile make up the finite element model. The length, width, and depth of a soil block are 12x12x15 metres, while the cross-section of a pile is 1 metre broad and 18 metres high. For both the front and back of the symmetrical plane, x-axis motion restricted. The model can only be rotated around the z-axis at the base. The study's FE model contains a total of 882 elements; 864 of these are located in the soil block and just 18 are located in the pile. To avoid volume locking due to undrained loading, C3D8R (eight-node linear hexahedral) elements with reduced integration and hourglass control are used to model the soil block and pile. To avoid wave reflection from the boundaries during seismic loading, an infinite element method is used to model the unbounded region (Saleh Asheghabadi and Ali 2020). The interior region is built with C3D8R, while the outer region is built with CIN3D8 (eight-node linear one-way infinite elements). The surface-to-surface contact interaction feature is used to model the soil-pile interface behaviour. The penalty method with a friction factor of 0.2 is used to simulate the interaction between soil and pile. An isotropic linear elastic model with Young's modulus E= 68.5 GPa, Poisson's ratio ν=0.32, and density=2700 kg/m^3 is considered for the pile, while the SS08 model enhanced with breakage is implemented in ABAQUS as a user defined interface. Loading is accomplished in three stages. The soil is subjected to a geostatic (gravity) load in the first step, and a superstructure mass of 1200 kg is applied on top of the pile in the second. Because the location of the earthquake time-history is not mentioned in Cheng and Jeremić (2009). As a result, a parametric study was conducted by changing the position of the acceleration time-history. When the time history is applied at a depth of 13.5 m below the ground surface, the model response matches well with Cheng's study.

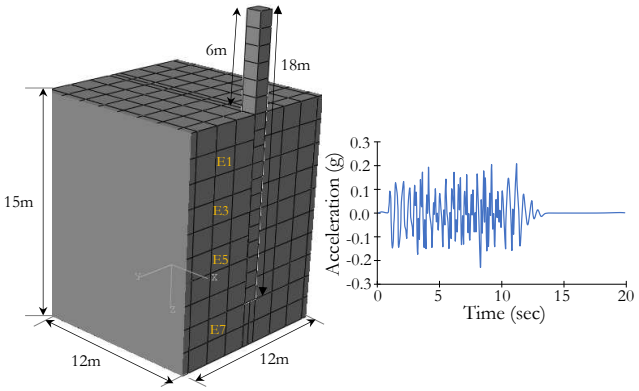

Figure 3. Geometry of the 3D finite element model with the acceleration time history.

The increment of the total stress is computed by

$$\dot{\sigma}_{ij} = L_{ijkl}\dot{\varepsilon}_{kl} - \dot{u}\delta_{ij} \quad (5)$$

where δ_{ij} is the Kronecar delta. During the undrained conditions, the locally volumetric deformation will be zero. Therefore, the change in void volume fraction ,

$$\frac{\dot{m}}{\rho_w} = \dot{\varepsilon}_{kl}\delta_{kl} + \frac{\dot{u}}{\overline{K}_w} = 0 \quad (6)$$

where, $\dot{m}$ represents the mass change in water per unit void volume fraction; ρ_w is the mass density of water; and $\overline{K}_w$ represents the bulk stiffness of water per unit void volume fraction. Substituting the pore water pressure change given in Equation (6), the stress increment in Equation (5) will be,

$$\dot{\sigma}_{ij} = L^{u}_{ijkl}\dot{\varepsilon}_{kl} \quad (7)$$

where, $L^{u}_{ijkl} = L_{ijkl} + \bar{K}_w\delta_{ij}\delta_{kl}$. In the present study, $\bar{K}_w = 10^7$ kPa is considered.

3.1 *Effectiveness of infinite element in the FEM model*

There are linear infinite elements in Abaqus/CAE that can be used to simulate the soil's infinite extent. When modelling with infinite elements, the region modelled with finite elements is referred to as the near-field region, while the far-field region is comprised of infinite elements. The benefit of using infinite elements at the boundary rather than only finite elements is that the geometry of the soil can be reduced while the soil boundaries do not influence the model response. A further advantage is that there is no need to implement a boundary condition at the boundary, as the infinite element itself acts as a boundary condition, with the displacement decreasing linearly within the element and reaching zero at the infinite boundary. To determine the efficacy of infinite elements at the boundary, a systematic parametric analysis is performed. Three cases (I, II and III) are considered shown in Figure 4, two (case I and case II) of which have the same dimensions as shown in Figure 3. One with a fixed boundary and the other with an infinite element. The third case (case III) is considered by increasing the soil domain three times on each side of the pile for better model response with fixed boundary. The primary objective was to see the effect of the boundary, so the soil considered here is linearly elastic with the values given in the preceding section, while keeping all other steps the same as in the previous section. Response of all cases as depicted in Figure 5 by comparing the lateral normal stress (S22) at 3.3m from the pile over a vertical distance of 12m. In comparison to Case I with a fixed boundary, Case II with infinite elements at the boundary and a large domain response is excellent. Looking at the results, case I response shows that soil domain with fixed boundary has a marginal effect on the results. It has been noticed that with infinite elements, the computational cost is significantly reduced.

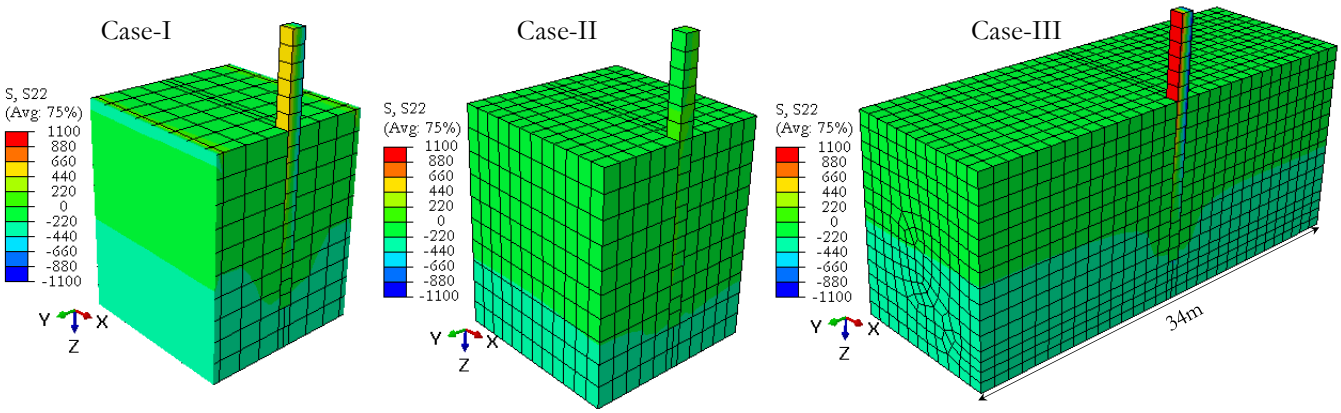

Figure 4. Contours of all three computed lateral normal stress cases in kPa .

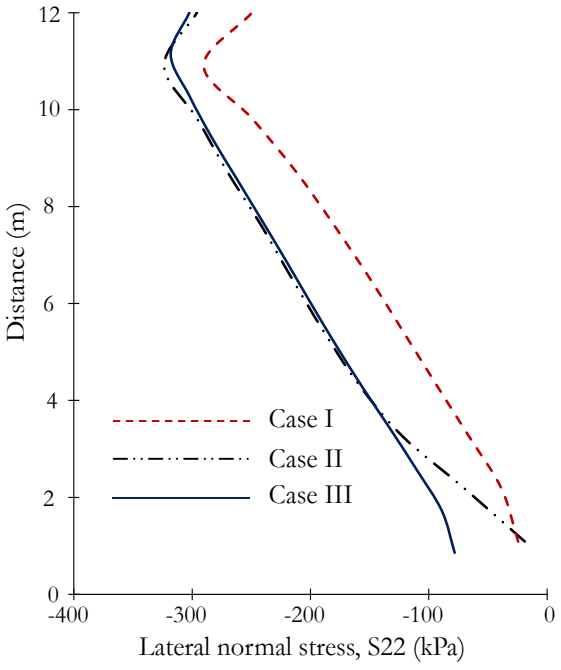

Figure 5. Lateral stress of all the cases with distance.

3.2 *FEM Validation*

The simulation response reported by Cheng and Jeremić (2009) is used to validate the FE model. In this study, the pile with a free column head on horizontal ground is used to validate the FE model. Since Toyoura sand is assumed to be non-crushable in Cheng and Jeremic's FEM model. Because of this, the FEM model is validated without taking the particle breakage effect into account. As a result, in the validation exercise, $e_{ref0} = e_{refu}$ is taken into account. Equation (8) gives the excess pore water pressure ratio R_u. It should be noted that the model response reported in Cheng and Jeremić (2009) study in terms of bending moment and excess pore water pressure ratio are taken into account for

validation. However, only the excess pore water pressure response is reported.

$$R_u = \frac{p'_{initial} - p'_{current}}{p'_{initial}} \quad (8)$$

where $p'_{initial}$ represents the mean effective stress prior to the seismic excitation and $p'_{current}$ represents the mean effective stress at any given time during the seismic excitation. Figure 6 compares R_u with time histories for two elements E5 and E7 . It should be noted that the model response is in good agreement with Cheng and Jeremić (2009) study, particularly for the deeper-depth soil.

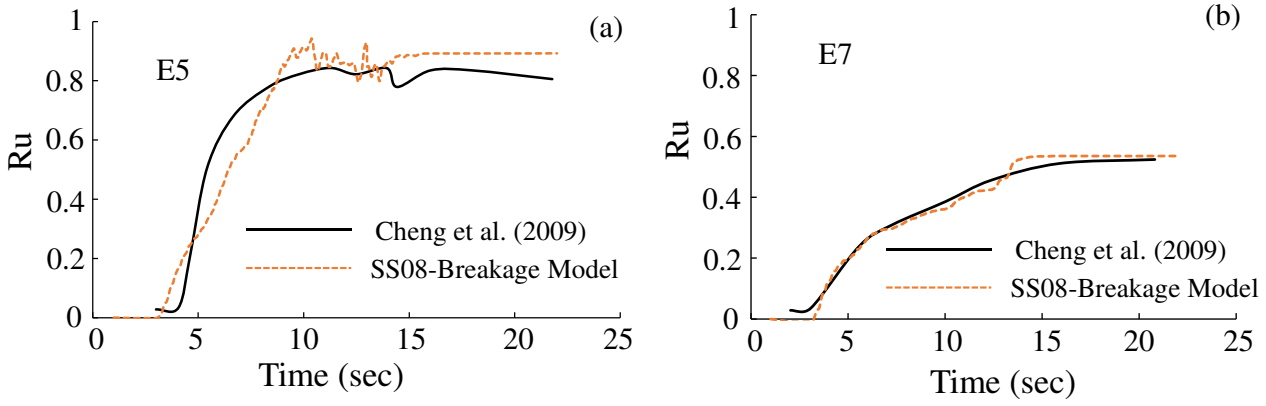

Figure 6. R_u time histories for elements E5 and E7.

4 EFFECT OF PARTICLE BREAKAGE

A comprehensive sensitivity analysis is carried out to determine how particle crushing affects the liquefaction potential during seismic loading. The crushing prospect of Toyoura sand is enhanced in the first part by taking reducing the breakage index, χ, while the other parameters remain unchanged. The acceleration time history considered here is the ground motion given in Cheng and Jeremić (2009) with a magnitude of 0.2g shown in Figure 3, in order to investigate the crushing effects further. Figure 7 depicts the evolution of the excess pore pressure ratio (R_u) envelope with depth for two scenarios (with and without breakage circumstances) at different time steps to better highlight the effects of particle crushing on the liquefaction potential. The comparison shows that particle breakage has a minor effect on the pore pressure response during the first few seconds of earthquake loading. However, the equivalent excess pore water ratio increases noticeably along the pile depth after only 6 seconds of loading. The excess pore water pressure ratio increased from 0.43 to 0.83 at the top surface, while the excess pore water pressure increased from 0.04 to 0.26 at a depth of 12m. It should be noted that after 15 seconds of time history, all of the elements up to a depth of 9m of pile reach a value of 0.94, however without particle crushing, the average value of excess pore water pressure is significantly lower. Higher confinement as we move from top to bottom results in more particle crushing and a consequent increase in pore pressure. It can be deduced that particle crushing increases the susceptibility to liquefaction by increasing the excess pore water pressure ratio. A comprehensive parametric study was carried out, and it was revealed that liquefaction resistance decreases as particle breakage increases due to sand softening, resulting in a decrease in hardening modulus (Saqib et al. 2022). Several other researchers agree with this finding. According to several cyclic triaxial experiment studies (Bouckovalas et al. 2003; Lade et al. 1997, 1998), increase in non-plastic fines in soil reduce liquifaction resistance.

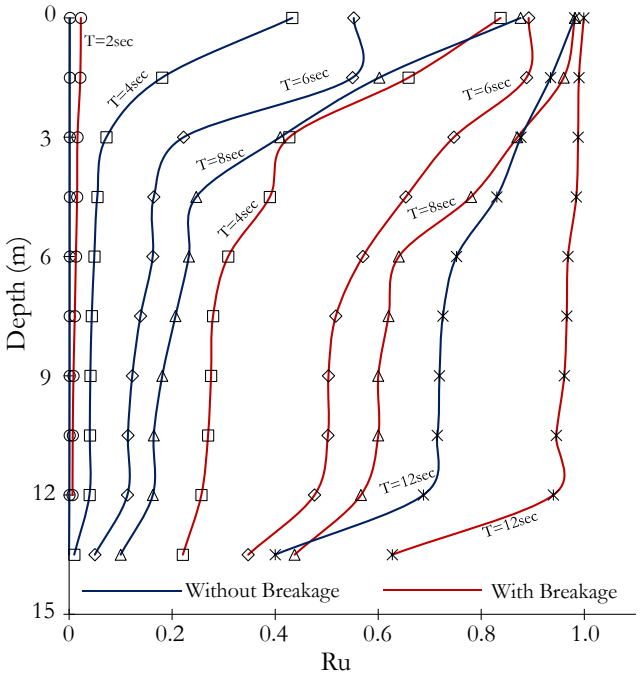

Figure 7. Effect of particle breakage on the evolution of the excess pore water pressure ratio

5 CONCLUSIONS

In this study, the behaviour of piles in crushable sand under seismic loading is predicted using a 3D finite element analysis. The bounding surface model enhanced with breakage is utilized and implemented in ABAQUS with a user-defined material interface. The performance of the FEM model is validated using data available in literature. Finally, a sensitivity analysis is performed on a pile with a free column head on horizontal ground to investigate the effect of particle crushing subjected to seismic loading. Simulated data shows that particle breakage raises the excess pore water pressure ratio, which in turn raises the susceptibility to liquefaction. Breakage occurs in the early stages of seismic loading when effective confinement is high. The particle breakage rate decreases as pore water pressure rise quickly due to excessive breakage.

5 ACKNOWLEDGEMENTS

The authors would like to express their gratitude to the Council of Scientific and Industrial Research, CSIR, 22(0732)/17/EMR-II, Arghya Das for financial support for this study.

6 REFERENCES

Bouckovalas, G. D., Andrianopoulos, K. I., and Papadimitriou, A. G. (2003). "A critical state interpretation for the cyclic liquefaction resistance of silty sands." 23, 115–125.

Cheng, Z., and Jeremić, B. (2009). "Numerical modeling and simulation of pile in liquefiable soil." *Soil Dynamics and Earthquake Engineering*, 29(11–12), 1405–1416.

Dafalias, Y. F., and Manzari, M. T. (2004). "Simple plasticity sand model accounting for fabric cahnge effects." *Journal of engineering mechanics*, 130(June), 622–634.

Einav, I. (2007). "Breakage mechanics-Part I: Theory." *Journal of the Mechanics and Physics of Solids*, 55(6), 1274–1297.

Galavi, V., Petalas, A., and Brinkgreve, R. B. J. (2013). "Finite element modelling of seismic liquefaction in soils." *Geotechnical Engineering*, 44(3), 55–64.

Ghafghazi, M., Shuttle, D. A., and DeJong, J. T. (2014). "Particle breakage and the critical state of sand." *Soils and Foundations*, Elsevier, 54(3), 451–461.

Hu, W., Yin, Z., Dano, C., and Hicher, P. Y. (2011). "A constitutive model for granular materials considering grain breakage." *Science China Technological Sciences*, 54(8), 2188–2196.

Hyodo, M., Wu, Y., Aramaki, N., and Nakata, Y. (2017). "Undrained monotonic and cyclic shear response and particle crushing of silica sand at low and high pressures." *Canadian Geotechnical Journal*, 54(2), 207–218.

Irani, N., Lashkari, A., and Tafili, M. (2022). "A state-dependent hyperelastic-plastic constitutive model considering shear-induced particle breakage in granular soils." *Acta Geotechnica*, Springer Berlin Heidelberg, 0123456789(i).

Lade, P. V., Liggio, C. D., and Yamamuro, J. A. (1998). "Effects of Non-Plastic Fines on Minimum and Maximum Void Ratios of Sand." *Geotechnical Testing Journal*, 21(4), 336–347.

Lade, P. V., Yamamuro, J. A., and Bopp, P. A. (1997). "Significance of Particle Crushing in Granular Materials." *Journal of Geotechnical and Geoenvironmental Engineering*, 123(9), 889–890.

Li, X. S., and Wang, Y. (1998). "Linear Representation of Steady-State Line for Sand." *Journal of Geotechnical and Geoenvironmental Engineering*, 124(12), 1215–1217.

Liu, H. Y., Abell, J. A., Diambra, A., and Pisanò, F. (2019). "Modelling the cyclic ratcheting of sands through memory-enhanced bounding surface plasticity." *Geotechnique*, 69(9), 783–800.

Manzari, M. T., and Dafalias, Y. F. (1997). "A critical state two-surface plasticity model for sands." *Geotechnique*, 47(2), 255–272.

Petalas, A. L., Dafalias, Y. F., and Papadimitriou, A. G. (2019). "SANISAND-FN: An evolving fabric-based sand model accounting for stress principal axes rotation." *International Journal for Numerical and Analytical Methods in Geomechanics*, 43(1), 97–123.

Rahimi, M., Chan, D., and Nouri, A. (2017). "Constitutive model for cyclic behaviour of cohesionless sands." *Geomechanics and Geoengineering*, Taylor & Francis, 12(1), 36–47.

Saleh Asheghabadi, M., and Ali, Z. (2020). "Infinite element boundary conditions for dynamic models under seismic loading." *Indian Journal of Physics*, Springer India, 94(6), 907–917.

Saqib, M., Das, A., and Patra, N. R. (2022). "A Constitutive Model for Cyclic Loading Response of Crushable." *Indian Geotechnical Journal*, Springer India.

Sloan, S. W., Abbo, A. J., and Sheng, D. (2001). "Refined explicit integration of elastoplastic models with automatic error control." *Engineering Computations*, 18(1), 121–154.

Taiebat, M., and Dafalias, Y. F. (2008). "SANISAND: Simple anisotropic sand plasticity model." *International Journal for Numerical and Analytical Methods in Geomechanics*, 32(8), 915–948.

Tengattini, A., Das, A., and Einav, I. (2016). "A constitutive modelling framework predicting critical state in sand undergoing crushing and dilation." *Geotechnique*, 66(9), 695–710.

Wang, R., Fu, P., and Zhang, J. M. (2016). "Finite element model for piles in liquefiable ground." *Computers and Geotechnics*, Elsevier Ltd, 72, 1–14.

Wang, R., Zhang, J. M., and Wang, G. (2014). "A unified plasticity model for large post-liquefaction shear deformation of sand." *Computers and Geotechnics*, Elsevier Ltd, 59, 54–66.

Wobbes, E., Beuth, L., Vuik, C., and Stolle, D. (2017). "No Title." *Procedia Engineering*, 175, 349–356.

Wood, D. M., and Maeda, K. (2008). "Changing grading of soil: Effect on critical states." *Acta Geotechnica*, 3(1), 3–14.

Xiao, Y., Wang, C., Zhang, Z., Liu, H., and Yin, Z. (2021). "Constitutive Modeling for Two Sands under High Pressure." *IJOG*, 21(5), 1–22.